

SUPPORTING INFORMATION

High-Resolution Bubble Printing of Quantum Dots

*Bharath Bangalore Rajeeva^{1,‡}, Linhan Lin^{1,‡}, Evan P. Perillo², Xiaolei Peng¹, William W. Yu³,
Andrew K. Dunn², Yuebing Zheng^{1,*}*

¹Materials Science and Engineering Program, Department of Mechanical Engineering, The University of Texas at Austin, Austin, Texas 78712, United States.

²Department of Biomedical Engineering, The University of Texas at Austin, Austin, Texas 78712, United States.

³Department of Chemistry and Physics, Louisiana State University, Shreveport, Louisiana LA 71115, United States.

[‡]These authors contributed equally to this work.

*E-mail: zheng@austin.utexas.edu

Table of Contents

Figure S1: Analysis of nanoparticle distribution on the plasmonic substrate

Figure S2: Optical properties of the rigid and flexible plasmonic substrate

Figure S3: Bubble dissolution process analyzed through the time stamp of the video frames

Figure S4: Dependence of linewidth on incident laser intensity

Figure S5: Large area patterning with various linespacing leading to quantum dot (QD) density modification.

Figure S6: High-resolution two-photon fluorescence image and analysis of structures resembling individual pixels.

Figure S7: Fluorescence stability and surface roughness of patterned QDs.

Figure S8: Bubble generation in various QD solutions.

Figure S9: Images of complex patterns created via bubble printing.

Figure S10: High-resolution patterning, surface roughness and emission properties of QDs patterned on flexible PET film.

Figure S11: Relative intensity plots of yellow QDs after fluorescence modification via BP.

Figure S12: Schematic of the optical setup used for fluorescence lifetime imaging (FLIM)

Figure S13: Fluorescence lifetime imaging microscopy images and surface profile of printed QDs.

Figure S14: The histogram and Gaussian fits of the lifetime of QDs patterned at various powers.

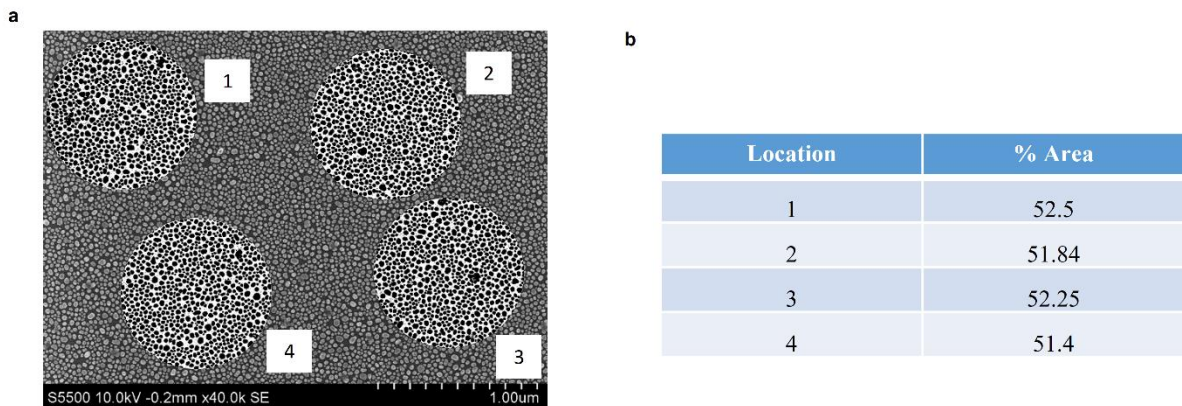


Figure S1: (a) SEM image of the plasmonic substrate for bubble printing. Spots of 940 nm in diameter were randomly chosen on the image, and the %area coverage of the AuNPs was calculated as shown in the table. (b) All spots show uniform AuNP coverage with a standard deviation of 0.54%.

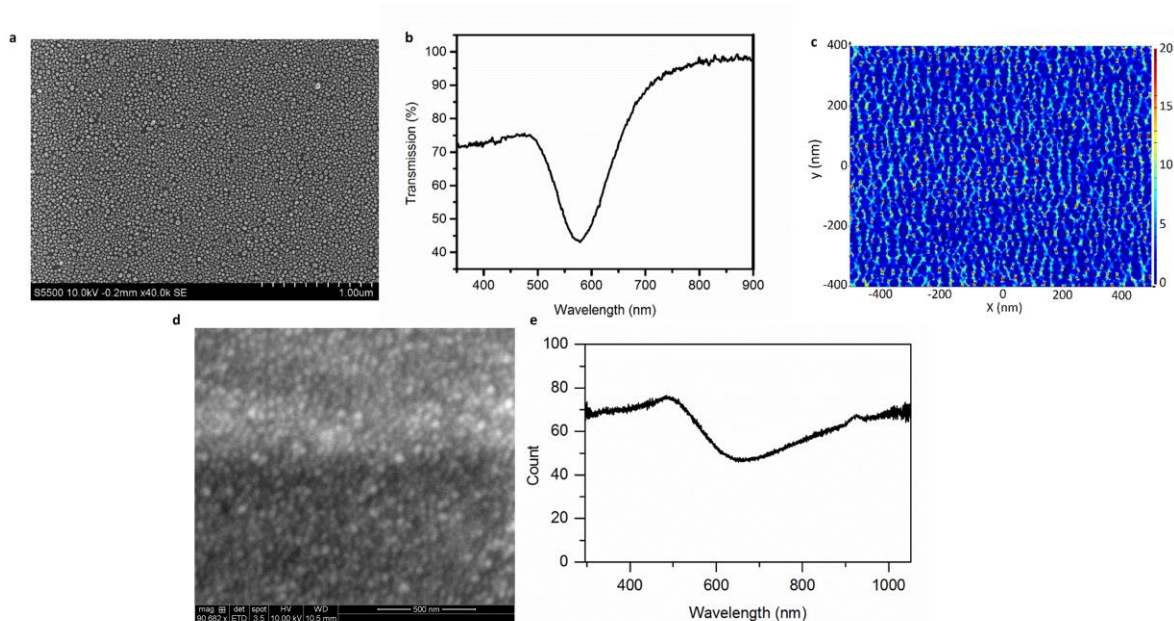


Figure S2: (a) SEM image of the plasmonic substrate. (b) Optical transmission spectrum of the substrate taken by Ocean Optics spectrometer. (c) Finite-difference time-domain (FDTD) simulation of the substrate shows a uniform distribution of hot spots, which leads to equivalent temperature rise at each location. (d) SEM image of the non-annealed 4 nm Au film on PET film shows a discontinuous film. (e) Optical transmission spectrum of non-annealed Au film showing a broad plasmonic resonance due to the higher particle-size heterogeneity.

FDTD simulations

The electromagnetic simulations were performed using the software package: FDTD Solutions, Lumerical Solutions. The plasmonic substrate was imported from a high-resolution SEM image, and the mesh size was chosen as 1nm. The refractive index (RI) of glass substrate was 1.52, and optical constants of Au were obtained from Johnson and Christy.¹ Perfectly matched layers were used as boundary conditions in all directions. The field distribution was recorded at green excitation (532 nm), which matches the wavelength of laser used in the experiments.

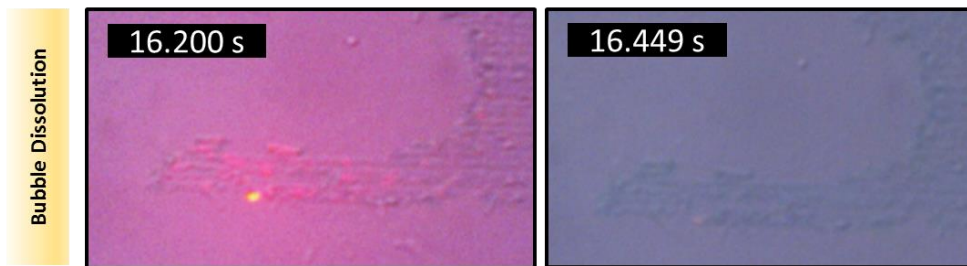


Figure S3: The bubble dissolution process is analyzed based on the video frames. The time taken for a bubble to dissolve completely is ~ 250 ms, which is obtained by subtracting the time stamps of the two frames. The video was taken at a frame rate of 50 frames/sec.

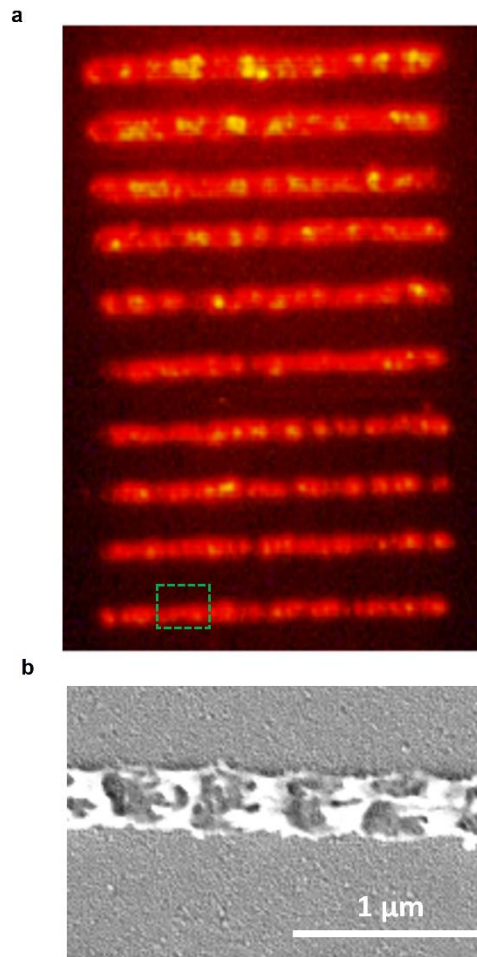


Figure S4: (a) Merged fluorescence image of the patterned lines of QDs demonstrating the linewidth variation in response to change in the incident laser power (Figure 2a). (b) SEM of the patterned line of QDs with a linewidth of 680 nm.

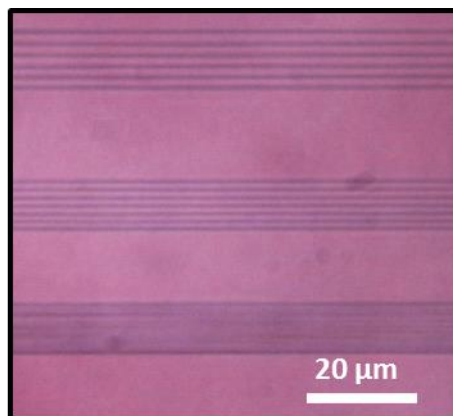


Figure S5: Large area patterning of QD rectangles created using BP with various line spacing. The line spacing is 1 μm , 1.5 μm , and 2 μm (bottom to top). The increase in line spacing results in a decrease in density of QDs, which manifests as a reduction in the fluorescence counts.

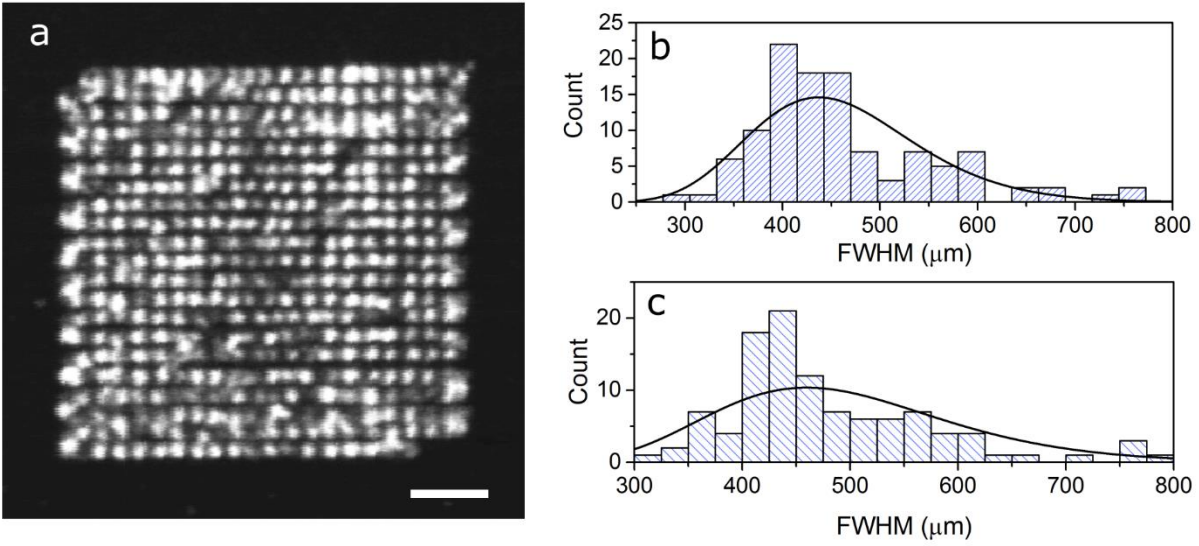


Figure S6: (a) High-resolution two-photon fluorescence image which resemble individual pixels. The dimension of each bright spot was calculated from the image, along both the x-axis and y-axis. (b, c) The width of each pixel is obtained by calculation of the FWHM of the spots based on the intensity. The values of FWHM from each spot is plotted in the histogram to obtain the size distribution. The mean of the distribution obtained via Gaussian fit is 450nm. The pixelated image is observed due to the crowding of QDs at edge of the bubble.

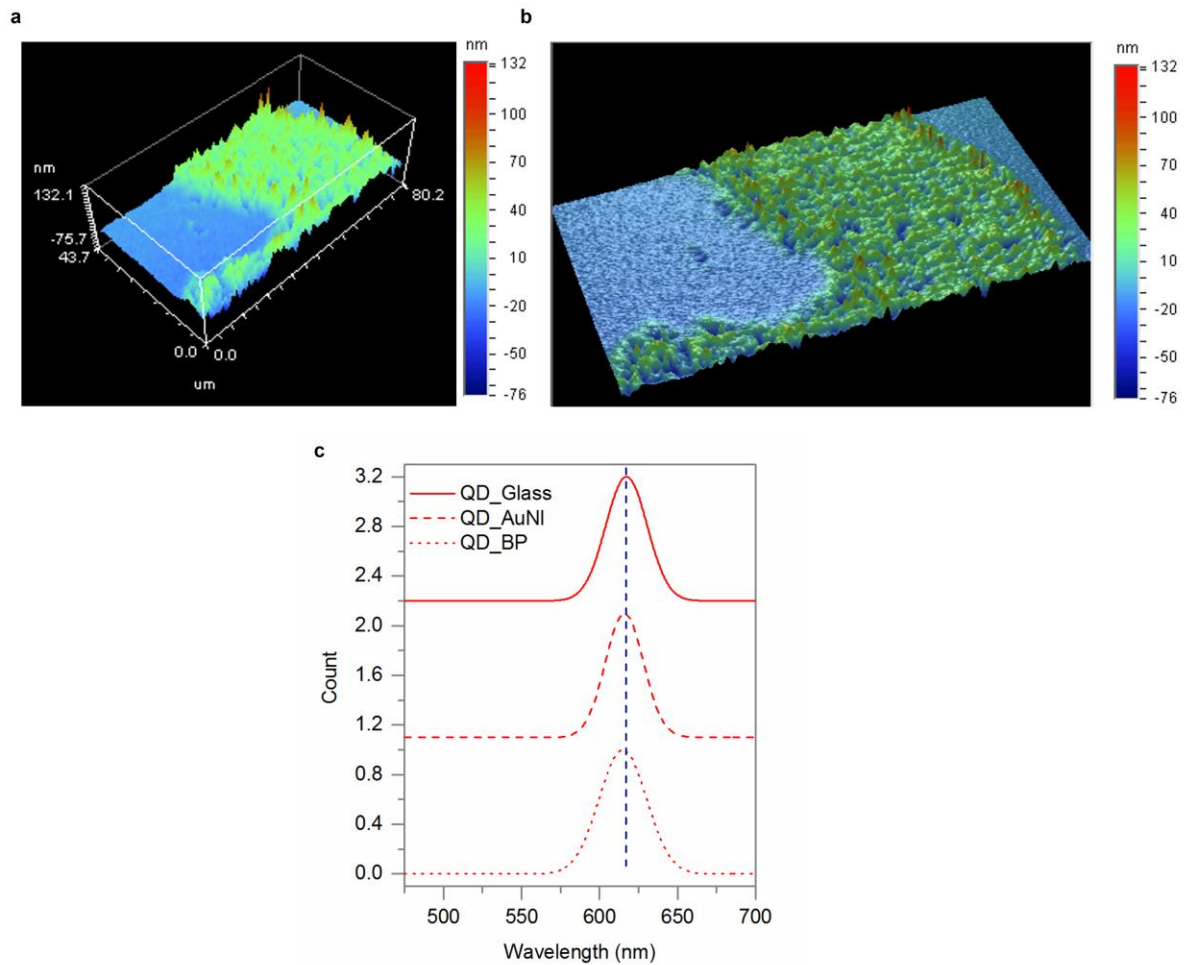


Figure S7: (a, b) Optical profilometry images of a $40 \mu\text{m} \times 80 \mu\text{m}$ region around the right eye of the Mona Lisa pattern (Figure 2d). The average and rms roughness of the printed QDs are 12.6 nm and 16.5 nm, respectively. (c) Emission spectrum of control QDs drop-casted on glass and AuNI (FWHM=30.2 nm), along with printed QDs (FWHM=34.1 nm). The printed QDs showed a blue-shift of ~ 1 nm, and FWHM increase of 3.9 nm.

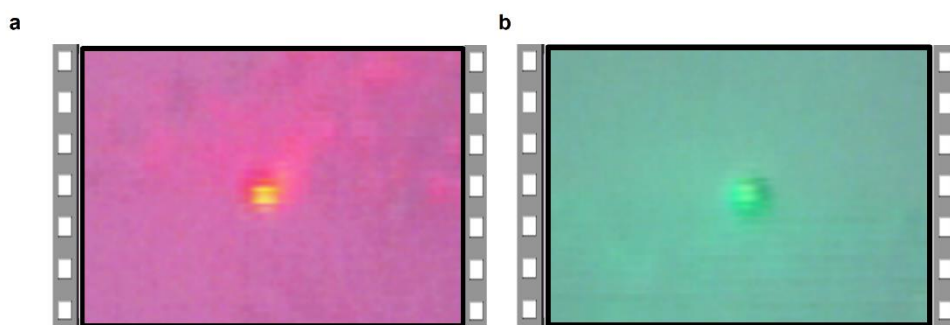


Figure S8: Optical images of bubbles generated at the interfaces of plasmonic substrates and QD solutions. (a) red QD solutions and (b) green QD solutions. The bubble generation is due to the photothermal heating of the plasmonic substrates.

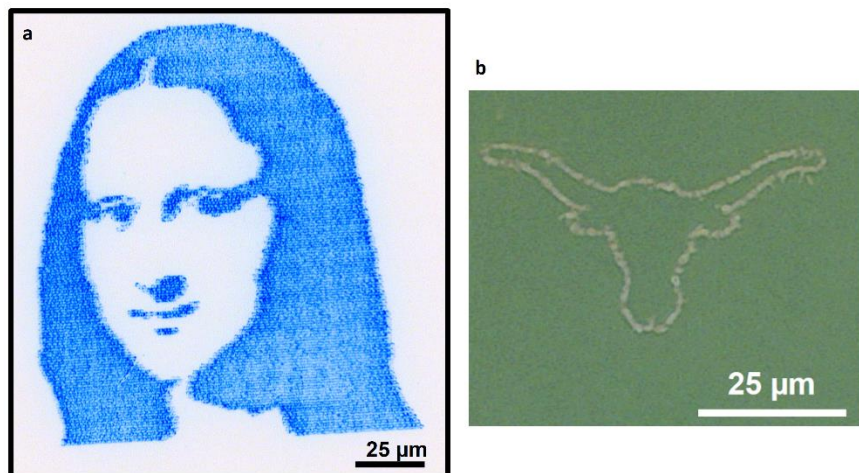


Figure S9: (a) Bright-field image of the yellow quantum dots patterned at a high stage speed of 10^{-2} m/s. (b) Bright-field image of contour of longhorn bubble printed with red QDs.

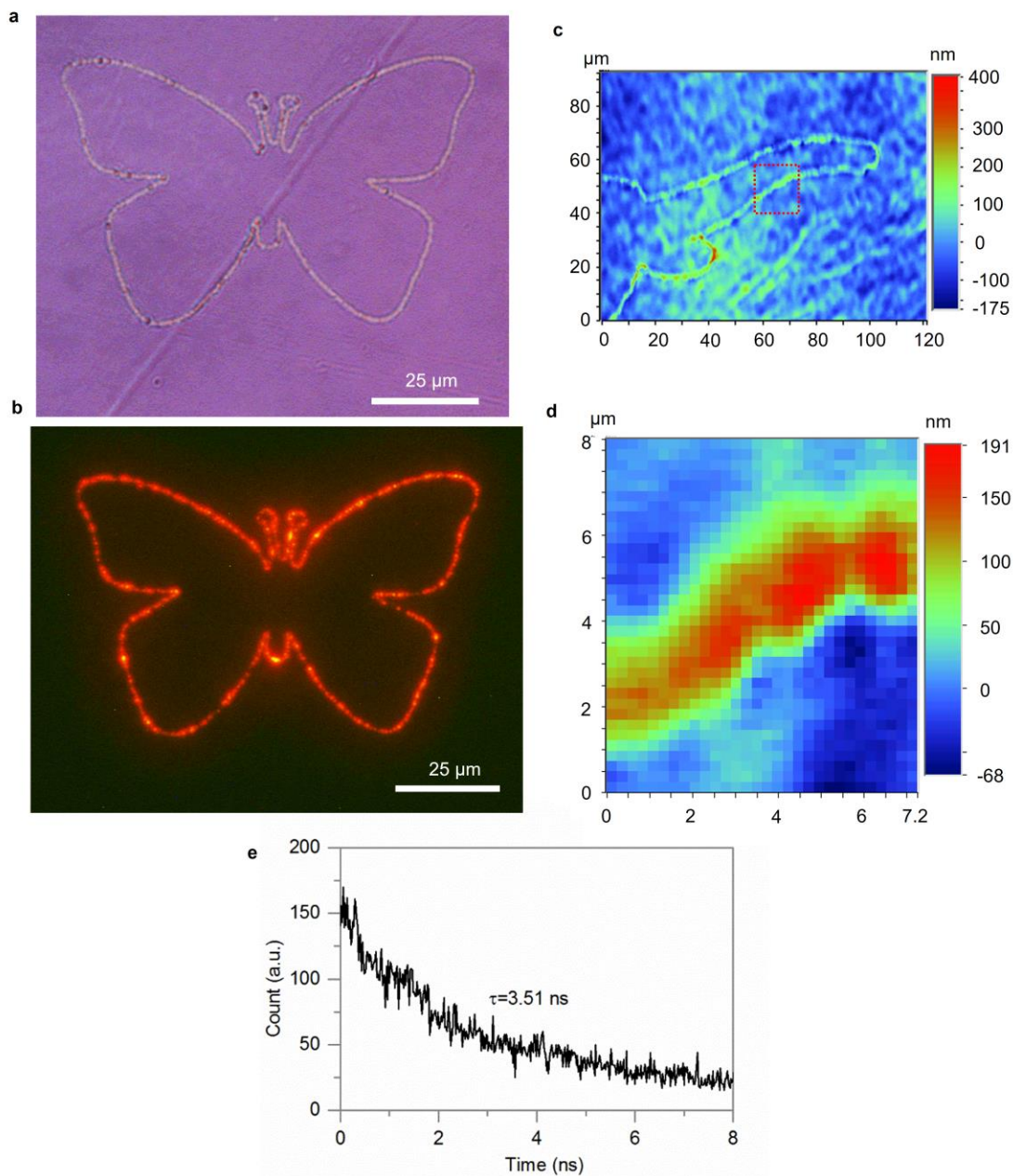


Figure S10: (a) Printing of QDs with sub-micron resolution on a PET film. The bump on the flexible substrate is also visible in the bright-field image. (b) Corresponding fluorescence image. (c) Optical profilometer image of the patterned longhorn, along with zoomed-in portion (d) of the image. The images show no major deformation of the underlying PET substrate. (e) Fluorescence lifetime of the printed QD in Fig. S11a. The lifetime is not extremely low due to the higher size heterogeneity of the particles on PET film, which results in the smaller E-field enhancement.

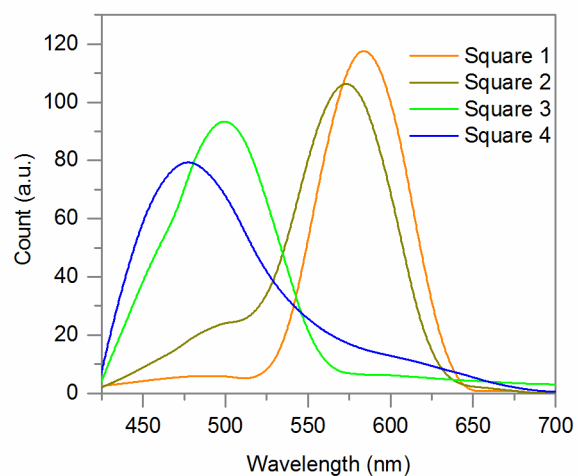


Figure S11: The relative intensity plots of the patterns fabricated in Fig. 5a. A relative decrease in the intensity of the QDs is observed with a progressive blue-shift. However, it is worth noting that the relative PL intensities do not provide a true metric since the absorbance of the blue vs. yellow QDs vastly differs, with the blue QDs expected to have much lower absorbance.² In addition, the concentration of QDs among the various squares isn't the same.

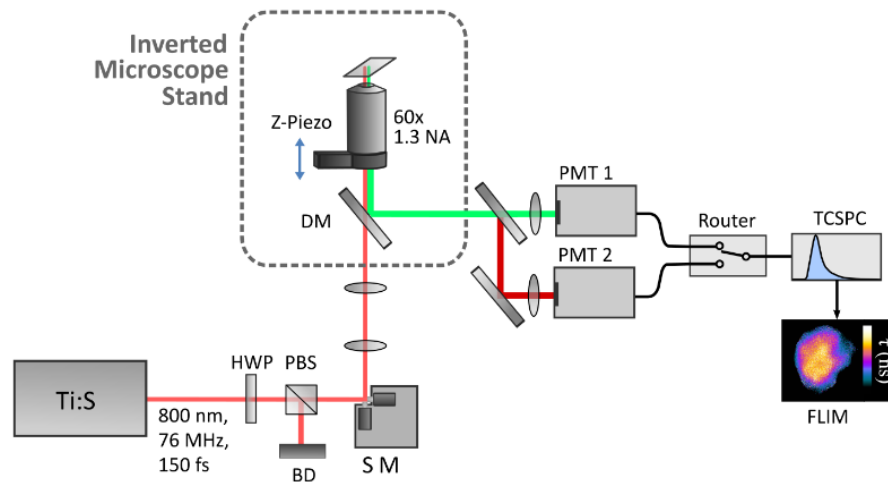


Figure S12: Schematic of optical setup for fluorescence-lifetime imaging microscopy (FLIM). PBS: Polarizing beam splitter, BD: Beam dump, SM: Scanning mirrors, DM: Dichroic mirror, PMT: Photomultiplier tube, and TCSPC: Time-correlated single-photon counting.

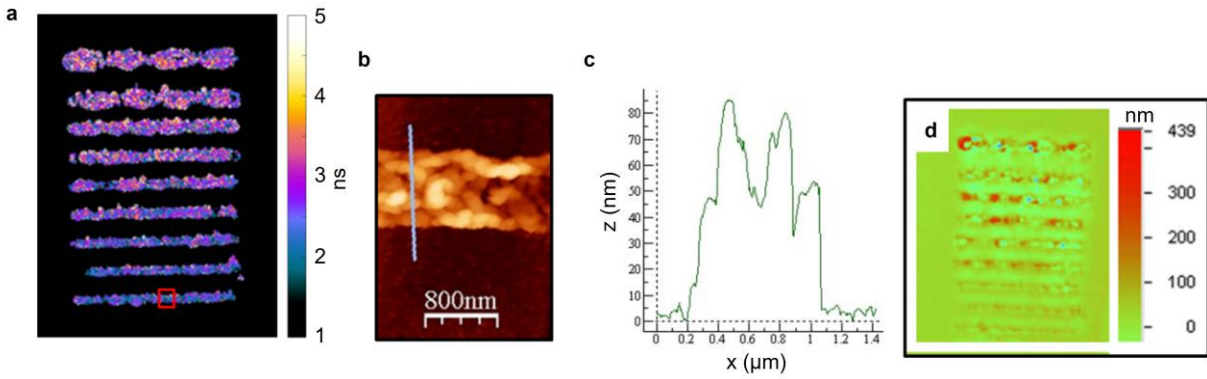


Figure S13: (a) FLIM image of the patterned QDs with increasing power. (b, c) AFM image and profile from the red region marked in (a). (d) optical profilometer image of (a). (b-d) The morphology changes with increase in the patterning parameters, with the height increasing from 80 nm to 440 nm. This alters the coupling intensity between the QDs and underlying plasmonic substrate.

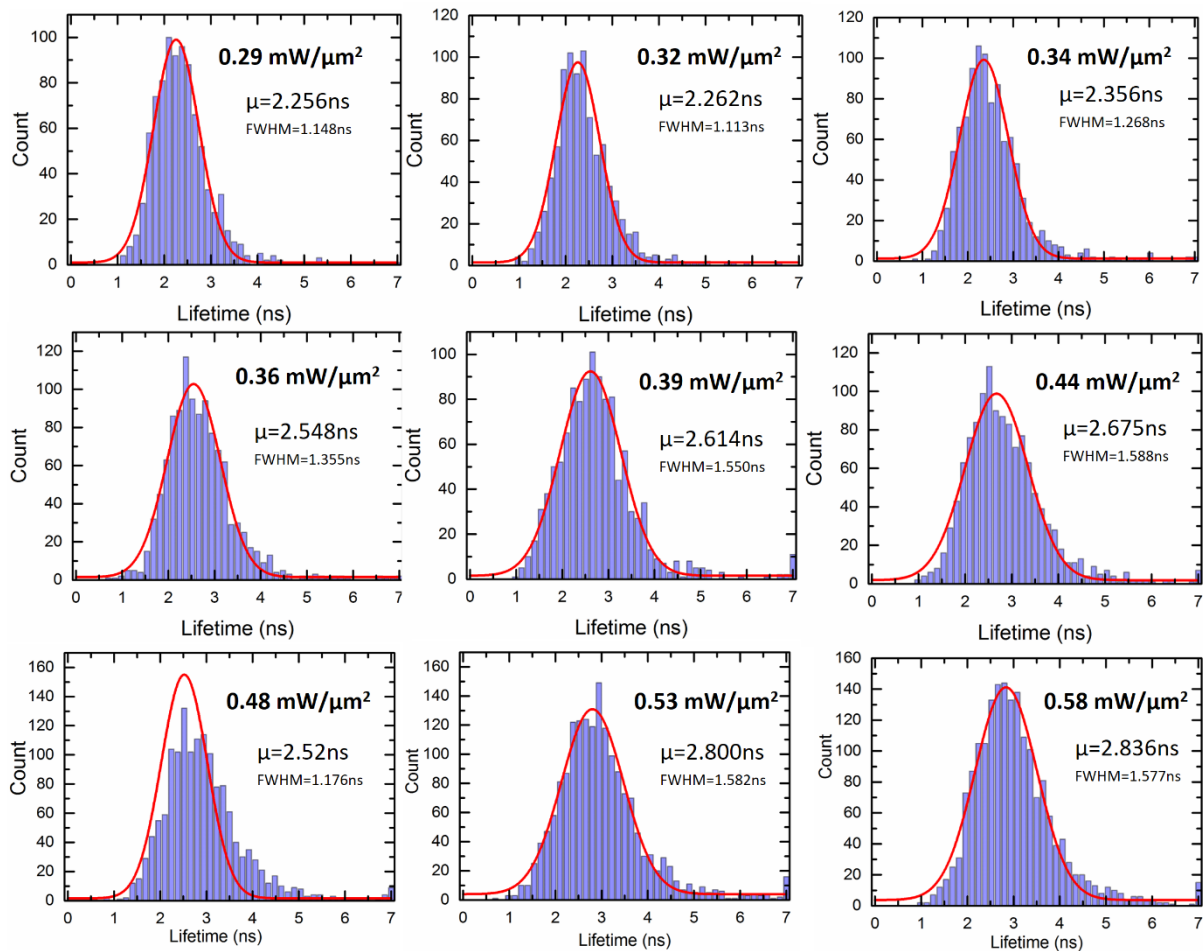


Figure S14: The histogram and Gaussian fitting of the lifetime of QDs patterned at various optical powers. Each histogram is obtained by isolating the lifetimes of individual lines patterned in Figure S13, and plotting them separately. For instance, the first histogram is obtained from the lifetime of all the pixels comprising the bottom most line in Figure S13. A gradual increase in the FWHM is observed as the power increases.

References

- (1) Johnson, P. B.; Christy, R.-W., Optical Constants of the Noble Metals. *Phys. Rev. B.* **1972**, *6* (12), 4370.
- (2) Dabbousi, B. O.; Rodriguez-Viejo, J.; Mikulec, F. V.; Heine, J. R.; Mattoussi, H.; Ober, R.; Jensen, K. F.; Bawendi, M. G., (CdSe)ZnS Core-Shell Quantum Dots: Synthesis and Characterization of a Size Series of Highly Luminescent Nanocrystallites. *J. Phys. Chem. B.* **1997**, *101* (46), 9463-9475.